

Spin liquid versus long range magnetic order in the frustrated body-centered tetragonal lattice

Carlene Farias

Univ. Bordeaux, LOMA, UMR 5798, F-33400 Talence, France

CNRS, LOMA, UMR 5798, F-33400 Talence, France

*International Institute of Physics, Universidade Federal do Rio Grande do Norte, 59078-400 Natal-RN, Brazil and
Departamento de Física Teórica e Experimental, Universidade Federal do Rio Grande do Norte, 59072-970 Natal-RN, Brazil*

Christopher Thomas

Instituto de Física, Universidade Federal do Rio Grande do Sul, 91501-970 Porto Alegre-RS, Brazil

Catherine Pépin

Institut de Physique Théorique, CEA-Saclay, 91191 Gif-sur-Yvette, France

Alvaro Ferraz

*International Institute of Physics, Universidade Federal do Rio Grande do Norte, 59078-400 Natal-RN, Brazil and
Departamento de Física Teórica e Experimental, Universidade Federal do Rio Grande do Norte, 59072-970 Natal-RN, Brazil*

Claudine Lacroix

*Institut Néel, Université Grenoble-Alpes, F-38042 Grenoble, France and
Institut Néel, CNRS, F-38042 Grenoble, France*

Sébastien Burdin

*Univ. Bordeaux, LOMA, UMR 5798, F-33400 Talence, France and
CNRS, LOMA, UMR 5798, F-33400 Talence, France*

(Dated: February 3, 2016)

An $SU(n)$ -symmetric generalization of the Heisenberg model for quantum spin S operators is used to investigate the geometrically frustrated body-centered tetragonal (BCT) lattice with antiferromagnetic interlayer coupling J_1 and intralayer first and second neighbor coupling J_2 and J_3 . Using complementary representations of the spin operators, we study the phase diagram characterizing the ground state of the system. For small n , we find that the most stable solutions correspond to four different families of possible long range magnetic orders that are governed by J_1 , J_2 , and J_3 . First, some possible instabilities of these phases are identified for $n = 2$ in large S expansions up to the linear spin-wave corrections. Then, using a fermionic representation of the $SU(n)$ spin operators for $S = 1/2$, we find that purely magnetic orders occur for $n \leq 3$ while spin-liquid (SL) solutions are stabilized for $n \geq 10$. The SL solution governed by J_1 breaks the lattice translation symmetry. This Modulated SL is associated to a commensurate ordering wave vector $(1, 1, 1)$. For $4 \leq n \leq 9$, we show how competition between J_1 , J_2 , and J_3 can tune the ground state from being magnetically ordered to a SL state. We discuss the relevance of this scenario for correlated systems with BCT crystal structure.

Introduction.—The body-centered tetragonal (BCT) lattice is one of the 14 three-dimensional (3D) lattice types.¹ This standard crystalline structure is realized in several strongly correlated electron materials with unusual magnetic and transport properties. Among the heavy fermion systems,^{2,3} different examples of materials with rare earth atoms on a BCT lattice have been intensively studied for the last decades: in URu_2Si_2 , a still mysterious Hidden order (HO) phase appears below the critical temperature $T_{HO} \approx 17$ K close to a pressure-induced antiferromagnetic (AF) transition;^{4,5} in $YbRh_2Si_2$ and $CeRu_2Si_2$, non-Fermi liquid properties are observed in the vicinity of AF quantum phase transitions, that are still poorly understood;^{6–9} $CeCu_2Si_2$ was the first heavy fermion material where unconventional superconductivity was discovered close to an AF transition;¹⁰ $CePd_2Si_2$ also exhibits unconventional superconductivity related to an AF transition;^{11,12} multi- Q AF order has been observed in $CeRh_2Si_2$.¹³ Today, each one of those “122” compounds can yet be considered as one entire field of research. It is noticeable that the link between AF ordering and unconventional

superconductivity has also been suggested in other families of correlated materials with BCT symmetry. In particular, the cuprate superconductors¹⁴ include among the AF insulating parent compounds La_2CuO_4 and $Sr_2CuO_2Cl_2$ in which the AF order originates from the Cu atoms that form a BCT crystal. However the relevant physics in their case is essentially two-dimensional (2D) with the BCT structure being involved only in the formation of the square-lattice layers of Cu atoms that order antiferromagnetically. Most of these materials are metals or superconductors, but their unconventional properties are strongly related to the interplay between charge and magnetic degrees of freedom. In this letter, our approach to these systems with itinerant electrons is orthogonal to several standard approaches since we will start from a localized point of view. We suggest that the rich diversity of unusual physical properties observed in these materials with BCT-structure is associated with the diversity of the underlying magnetic phases in competition.

Important theoretical developments were made in the past years on the unconventional magnetic properties of the BCT

lattice using a classical Heisenberg model, following the pioneering study by Villain.^{15–22}

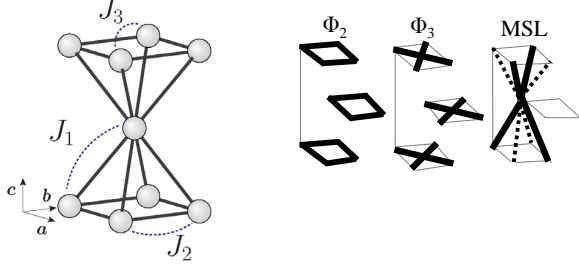


FIG. 1. Left: BCT lattice and the J_1 , J_2 , and J_3 interactions. In this letter, the tetragonal lattice constants are set to $a = b = c = 1$. Right: bold lines represent the three kinds of intersite SL correlations on the BCT structure.

Model.—In this letter, we analyze the ground states of an $SU(n)$ generalization of the J_1 - J_2 - J_3 quantum Heisenberg Hamiltonian introduced here first for $n = 2$:

$$H_{n=2}^S = \sum_{\langle \mathbf{R}, \mathbf{R}' \rangle} J_{\mathbf{R}\mathbf{R}'} \vec{S}_{\mathbf{R}} \cdot \vec{S}_{\mathbf{R}'}, \quad (1)$$

where $\vec{S}_{\mathbf{R}} \equiv (S_{\mathbf{R}}^x, S_{\mathbf{R}}^y, S_{\mathbf{R}}^z)$ denotes quantum spin S operators acting on site \mathbf{R} of a BCT-lattice. The antiferromagnetic interaction $J_{\mathbf{R}\mathbf{R}'}$ connects sites \mathbf{R} and \mathbf{R}' , and can take three possible values $J_1, J_2, J_3 > 0$, as indicated in figure 1.

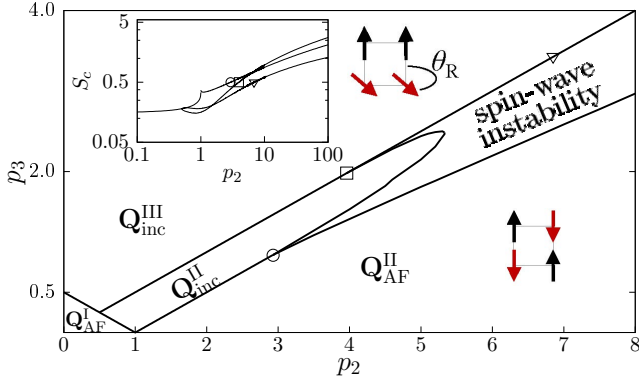


FIG. 2. (Color online) Classical ground state phase diagram of the J_1 - J_2 - J_3 model in coordinates (p_2, p_3) . The solid lines indicate transitions between the stable magnetic ordered states with modulating vectors $\mathbf{Q}_{\text{AF}}^{\text{I}}$, $\mathbf{Q}_{\text{AF}}^{\text{II}}$, $\mathbf{Q}_{\text{inc}}^{\text{II}}$, and $\mathbf{Q}_{\text{inc}}^{\text{III}}$. A schematic representation is provided for $\mathbf{Q}_{\text{AF}}^{\text{II}}$ and $\mathbf{Q}_{\text{inc}}^{\text{III}}$. The linear SW instability region is depicted here for $S = 1/2$. Inset: critical value S_c as a function of p_2 when p_3 is bound to the critical lines. The three symbols indicate the corresponding location of critical value $S_c = 1/2$ in each case.

Classical ground state.—Following the standard spin-wave (SW) approach, we start with the $S = +\infty$ generalization of the Hamiltonian (1), which corresponds to the limit of classical spins. For the sake of simplification, we consider only magnetic orderings that are characterized by a single wavevector $\mathbf{Q} = 2\pi(\lambda, \mu, \nu)$ identified as (λ, μ, ν) in reduced notations. Invoking Fourier transforms, this wavevector is used to

minimize the classical dispersion $J(\mathbf{q}) \equiv 8J_1\gamma_1^{\mathbf{q}} + 2J_2\gamma_2^{\mathbf{q}} + 4J_3\gamma_3^{\mathbf{q}}$, with

$$\gamma_1^{\mathbf{q}} \equiv \cos(q_x/2) \cos(q_y/2) \cos(q_z/2), \quad (2)$$

$$\gamma_2^{\mathbf{q}} \equiv \cos(q_x) + \cos(q_y), \quad (3)$$

$$\gamma_3^{\mathbf{q}} \equiv \cos(q_x) \cos(q_y). \quad (4)$$

Tuning the dimensionless parameters $p_2 \equiv J_2/J_1$ and $p_3 \equiv J_3/J_1$, we find that the ground state can be characterized by four kinds of possible wavevectors, as depicted in figure 2: $\mathbf{Q}_{\text{AF}}^{\text{I}} \equiv (1, 1, 1)$ and $\mathbf{Q}_{\text{AF}}^{\text{II}} \equiv (1/2, 1/2, \nu)$ correspond to the regimes where the Weiss field is dominated by J_1 and J_2 respectively. The ν -degeneracy in the latter case indicates the underlying bidimensionality. The other possible ordering wavevectors are incommensurate and characterize two kinds of helical orders: $\mathbf{Q}_{\text{inc}}^{\text{III}} \equiv (0, \Upsilon_3, 0)$ degenerate with $(\Upsilon_3, 0, 0)$, $(1, \Upsilon_3, 1)$, and $(\Upsilon_3, 1, 1)$ where $\Upsilon_3 = \frac{1}{\pi} \arccos \frac{-1}{p_2 + 2p_3}$; and $\mathbf{Q}_{\text{inc}}^{\text{II}} \equiv (\Upsilon_2, \pm \Upsilon_2, 1)$ degenerate with $(\Upsilon_2, 1 \pm \Upsilon_2, 0)$, where $\Upsilon_2 = \frac{1}{2\pi} \arccos \frac{1-p_2}{2p_3}$. A different wave-vector, $\mathbf{Q}_{\text{AF}}^{\text{III}} \equiv (0, 1/2, \nu)$ had been proposed²³ in a J_3 -dominated phase, which corresponds to the commensurate order characterizing a purely bidimensional square lattice. We find that $J_1 \neq 0$ corrections are relevant and $\mathbf{Q}_{\text{inc}}^{\text{III}}$ is energetically more stable than $\mathbf{Q}_{\text{AF}}^{\text{III}}$. Not surprisingly these two vectors are asymptotically identical at large p_3 . Similarly, $\mathbf{Q}_{\text{inc}}^{\text{II}} \mapsto \mathbf{Q}_{\text{AF}}^{\text{II}}$ at large p_2 . The transition lines separating these four classical phases are given by linear relations between p_2 and p_3 . The $\mathbf{Q}_{\text{inc}}^{\text{II}} - \mathbf{Q}_{\text{inc}}^{\text{III}}$ transition is discontinuous, the other transitions are continuous.

Order by quantum disorder.—Then, assuming a given classical ground state \mathbf{Q} , we study the large- S corrections. This expansion invokes a helical generalization of the Holstein-Primakov representation:^{16,19,24} introducing boson annihilation (creation) $a_{\mathbf{R}}^{(\dagger)}$, spin operators are approximated as $S_{\mathbf{R}}^x \approx (S/2)^{1/2}(a_{\mathbf{R}} + a_{\mathbf{R}}^{\dagger})$, and $\begin{pmatrix} S_{\mathbf{R}}^z \\ S_{\mathbf{R}}^y \end{pmatrix} \approx \begin{bmatrix} \cos \theta_{\mathbf{R}} & \sin \theta_{\mathbf{R}} \\ -\sin \theta_{\mathbf{R}} & \cos \theta_{\mathbf{R}} \end{bmatrix} \begin{pmatrix} S - a_{\mathbf{R}}^{\dagger} a_{\mathbf{R}} \\ -i(S/2)^{1/2}(a_{\mathbf{R}} - a_{\mathbf{R}}^{\dagger}) \end{pmatrix}$, with $\theta_{\mathbf{R}} \equiv \mathbf{Q} \cdot (\mathbf{R} - \mathbf{R}_0)$, where z is the easy axis characterizing a site \mathbf{R}_0 chosen arbitrarily. The dispersions obtained for the Bogoliubov quasiparticles are $\Omega_{\mathbf{k}}^+ \equiv J(\mathbf{k}) - J(\mathbf{Q})$ and $\Omega_{\mathbf{k}}^- \equiv \frac{J(\mathbf{k}+\mathbf{Q}) + J(\mathbf{k}-\mathbf{Q})}{2} - J(\mathbf{Q})$.

Whilst the ground state energy is proportional to $S^2 J(\mathbf{Q})$ at the highest order, the first correction is proportional to $S \int_{\text{BCT}} d^3 \mathbf{k} \sqrt{\Omega_{\mathbf{k}}^+ \Omega_{\mathbf{k}}^-}$ where the \mathbf{k} -integral runs over the first Brillouin zone of the BCT-lattice. Analyzing this correction for the classically degenerate vectors $\mathbf{Q}_{\text{AF}}^{\text{II}}$, we find that the resulting order is stabilized by quantum disorder: the continuous degeneracy is lift in favor of $\nu = 0$, which is equivalent to $\nu = 1$.

Fluctuation corrections to magnetization.—We also studied the effects of fluctuations emerging from the linear SW corrections. Generalizing to the BCT-structure the approach introduced in²⁵ for the square lattice model, the staggered magnetization is expanded around its classical value $\langle S_{\mathbf{R}_0}^z \rangle \approx$

$S - \Delta m(p_2, p_3)$. We find:

$$\Delta m(p_2, p_3) = \langle a_{\mathbf{R}_0}^\dagger a_{\mathbf{R}_0} \rangle = -\frac{1}{2} + \int_{\text{BCT}} \frac{d^3 \mathbf{k}}{64\pi^3} \frac{\Omega_{\mathbf{k}}^+ + \Omega_{\mathbf{k}}^-}{\sqrt{\Omega_{\mathbf{k}}^+ \Omega_{\mathbf{k}}^-}}, \quad (5)$$

Unlike the 2D case,²⁵ fluctuation corrections here do not diverge, which is not surprising with a 3D model. Frustration can relatively increase the critical value of S below which the linear spin-wave correction cancels the staggered magnetization, $S_c \equiv \Delta m(p_2, p_3)$. Indeed, for fixed p_2 , we find that S_c increases when p_3 approaches its critical value associated with the classical phase boundary. This maximal value is plotted in the inset of figure 2 as a function of p_2 for the continuous $\mathbf{Q}_{\text{AF}}^{\text{II}}/\mathbf{Q}_{\text{inc}}^{\text{II}}$ transition and on each side of the discontinuous $\mathbf{Q}_{\text{inc}}^{\text{II}}/\mathbf{Q}_{\text{inc}}^{\text{III}}$ transition. On each of these critical lines, we find $S_c \sim \sqrt{p_2}$ at large p_2 . Furthermore, a logarithmic $S_c \sim \ln(p_2/2 - p_3)$ and a power law $S_c \sim 1/\sqrt{p_3 - p_2/2}$ are respectively obtained at large p_2 in the vicinity of the $\mathbf{Q}_{\text{inc}}^{\text{II}} \rightarrow \mathbf{Q}_{\text{inc}}^{\text{III}}$ and $\mathbf{Q}_{\text{inc}}^{\text{III}} \rightarrow \mathbf{Q}_{\text{inc}}^{\text{II}}$ transitions. This result is consistent with the square lattice spin wave analysis.²⁵

Generalized $SU(n)$ symmetric model.—The SW approach thus reveals some weaknesses of the classical magnetic orders, but the three-dimensionality protects these states against small fluctuations at the lowest, linear, order. One may go further and study possible instabilities emerging from next orders, taking into account interactions between the spin-wave bosonic excitations. Hereafter, we follow an alternative approach: we analyze the possibility that the system forms a Resonant Valence Bond state with fermionic excitations and SL correlations.^{26,27} One of our physical motivations is driven by the physics of unconventional metallic systems with BCT structure: in several of these correlated systems, magnetic degrees of freedom seem to be “deconfined” into fermionic ones that may contribute to the formation of a Fermi-surface, unlike weakly coupled bosons. Such a scenario inspired by the physics of cuprate superconductors^{28–31} could be easily strengthened by a coupling of the Heisenberg spins of the J_1 - J_2 - J_3 model to extra charge degrees of freedom. In the following we will study this possible “fermionic deconfinement” of spin operators as an intrinsic property of the Heisenberg model. To this goal, considering $S = 1/2$, the Hamiltonian (1) is generalized to $SU(n)$ -symmetry:

$$H_n^{S=1/2} = \sum_{\langle \mathbf{R}, \mathbf{R}' \rangle} \frac{J_{\mathbf{R}\mathbf{R}'}}{n} \sum_{\sigma\sigma'} \chi_{\mathbf{R}\sigma}^\dagger \chi_{\mathbf{R}\sigma'} \chi_{\mathbf{R}'\sigma'}^\dagger \chi_{\mathbf{R}'\sigma}, \quad (6)$$

where $\chi_{\mathbf{R}\sigma}^{(\dagger)}$ ($\chi_{\mathbf{R}\sigma}$) are annihilation (creation) fermionic operators with orbital degeneracy $\sigma = 1, \dots, n$, and satisfying the local constraints $\sum_{\sigma} \chi_{\mathbf{R}\sigma}^\dagger \chi_{\mathbf{R}\sigma} = n/2$. This is a standard $SU(n)$ generalization³² of the fermionic representation developed by Abrikosov for $n = 2$. The scaling factor $1/n$ ensures that the energy remains extensive, i.e., proportional to n , in the large- n limit.

Spin-liquid correlations.—Using the Hubbard-Stratonovitch decoupling as described in,^{33,34} the low temperature phases of Hamiltonian (6) can be characterized by two kinds of order parameters: the local magnetization

field $m_{\mathbf{R}}^\sigma = \langle \chi_{\mathbf{R}\sigma}^\dagger \chi_{\mathbf{R}\sigma} \rangle - \frac{1}{2}$, and the intersite spin-liquid fields $\varphi_{\mathbf{R}\mathbf{R}'} = -\frac{1}{n} \sum_{\sigma} \langle \chi_{\mathbf{R}\sigma}^\dagger \chi_{\mathbf{R}'\sigma} \rangle$. The purely magnetic classical mean-field theory characterized here by a staggered magnetization $m_{\mathbf{R}}^\sigma = \pm S_{\mathbf{Q}}$ is equivalent to the one we analyzed for the $S = +\infty$ limit. The corresponding ground state phase diagram is thus given by figure 2. Hereafter, the stability of these classical magnetic orders is analyzed by testing various SL Ansätze as alternative possible ground states. Generalizing the Modulated SL (MSL) order introduced in,³⁴ we consider the nearest neighbor intersite correlations $\varphi_{\mathbf{R}\mathbf{R}'}^1 = \frac{1}{2} [\Phi_1 + i e^{i \mathbf{Q}_{\text{AF}}^{\text{I}} \cdot (\frac{\mathbf{R}+\mathbf{R}'}{2})} \Phi_M]$, $\varphi_{\mathbf{R}\mathbf{R}'}^2 = \Phi_2$, and $\varphi_{\mathbf{R}\mathbf{R}'}^3 = \Phi_3$ with a bond index definition similar to the one of figure 1. The free energy per spin component and per lattice site is expressed for each AF or SL state as:

$$F = F_0 - \frac{k_B T}{32\pi^3} \int_{\text{BCT}} d^3 \mathbf{k} \sum_{s=\pm} \ln \left(1 + e^{-\frac{E_{\mathbf{k}}^s}{k_B T}} \right) - \frac{\lambda_0}{2} \quad (7)$$

where λ_0 denotes a Lagrange multiplier that minimizes F in order to satisfy the constraint for the fermionic occupation. For the AF orderings, the zero-point energy is $F_0 = -\frac{2J(\mathbf{Q})}{n} |S_{\mathbf{Q}}|^2$ and the dispersion $E_{\mathbf{k}}^\pm = \lambda_0 \pm \frac{J(\mathbf{Q})}{n} S_{\mathbf{Q}}$. For the SL states we find $F_0/J_1 = |\Phi_1|^2 + |\Phi_M|^2 + 2p_2 |\Phi_2|^2 + 2p_3 |\Phi_3|^2$ and $(E_{\mathbf{k}}^\pm - \lambda_0)/J_1 = 2p_2 \gamma_2^{\mathbf{k}} \Phi_2 + 4p_3 \gamma_3^{\mathbf{k}} \Phi_3 \pm 4\sqrt{(\gamma_1^{\mathbf{k}} \Phi_1)^2 + (\gamma_M^{\mathbf{k}} \Phi_M)^2}$. Here, the non-BCT-periodic real term Φ_M with $\gamma_M^{\mathbf{k}} \equiv \sin(q_x/2) \sin(q_y/2) \sin(q_z/2)$ takes into account a possible spatial amplitude modulation of the SL field. Considering that this MSL is a BCT adaptation of the “kite” phase studied in³² for a square lattice, we also tested another non-homogeneous “flux” phase SL characterizing a chiral state with complex $\varphi_{\mathbf{R}\mathbf{R}'}^1 = (\varphi_{\mathbf{R}\mathbf{R}'}^1)^*$ that could be described within a very close formalism by simply replacing $\gamma_M^{\mathbf{k}} \rightarrow \sin(q_x/2) \sin(q_y/2) \cos(q_z/2)$. This chiral SL was found to have a higher energy than the MSL.

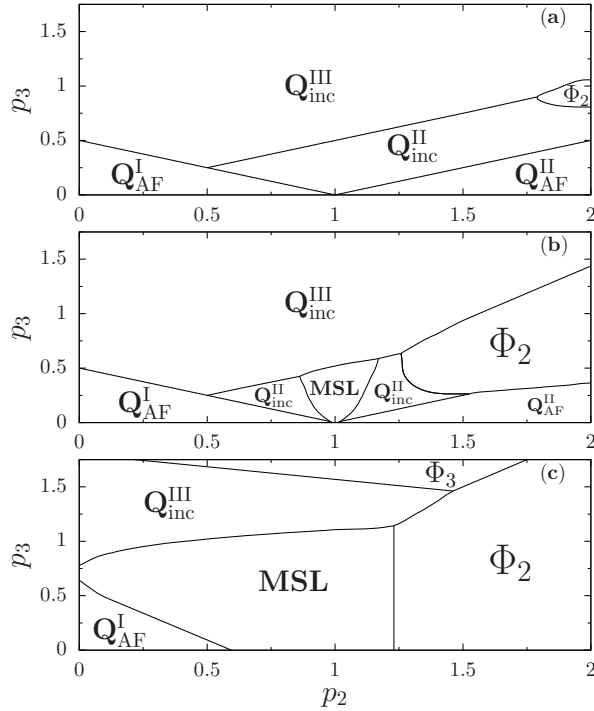


FIG. 3. Ground state phase diagram of the J_1 - J_2 - J_3 model in coordinates (p_2, p_3) obtained for $n = 4$ (a), 5 (b), 7 (c).

Phase diagram.—For $n \leq 3$ we find purely AF ground states, and for $n \geq 10$ the most stable states are SL characterized by finite values of either Φ_M , Φ_2 , or Φ_3 . At mean-field level, these three SL parameters do not coexist. Furthermore, we remark that the transition between the MSL and the Φ_2 -dominated SL phases is first order. Beyond mean-field, we expect that only the SL critical temperature associated with a non-zero Φ_M still corresponds to a phase transition signaled by the translation symmetry breaking. For $4 \leq n \leq 9$ we find a rich phase diagram exhibiting AF/SL quantum phase transitions that are controlled by J_1 - J_2 - J_3 parameters, as illustrated on figure 3. Increasing n , AF-SL instability shows up first within the Q_{inc}^{II} phase. Furthermore, comparing the large- S phase diagram (fig. 2) with the one obtained for $n = 4$ (fig. 3), one observes that the $S_c = 1/2$ spin-wave instability is located in the same region where the Φ_2 dominant state becomes stabilized. Also, beyond the specificity of the associated order parameters, figure 3 indicates that the SL instability “propagates” from large- p_2 (Φ_2) to smaller- p_2 (MSL) areas if we increase the value of n .

MSL phase for $S = 1/2$.—An interesting feature also appears for the MSL solution: with a relatively high numerical accuracy the modulation field Φ_M is found to be always equal to the homogeneous field Φ_1 . This leads to a very extreme situation for the inter-layer field $\varphi_{\mathbf{R}\mathbf{R}'}^1 = \frac{1}{2}[\Phi_1 \pm \Phi_M]$ which vanishes on half of the bonds while it keeps the finite value $\Phi_1 = \Phi_M$ on the other bonds. Introducing the probability $p_{\mathbf{R}\mathbf{R}'}^{singlet}$ that a given bond $\mathbf{R}\mathbf{R}'$ forms a singlet, the formation of the MSL state can be interpreted here as follows: first, for all the inter-layer bonds such that $\mathbf{Q}_{AF}^I \cdot (\mathbf{R} + \mathbf{R}')/2 = \pi/2$, the interaction terms are effectively decoupled at mean-field

level, leading to $p_{\mathbf{R}\mathbf{R}'}^{singlet} = 1/4$ and $\langle \vec{S}_{\mathbf{R}} \cdot \vec{S}_{\mathbf{R}'} \rangle = 0$. Then the SL with $\langle \vec{S}_{\mathbf{R}} \cdot \vec{S}_{\mathbf{R}'} \rangle \neq 0$ is formed on the other inter-layer bonds, with $\mathbf{Q}_{AF}^I \cdot (\mathbf{R} + \mathbf{R}')/2 = -\pi/2$, that remain effectively coupled. Using the numerical value $\Phi_1 = \Phi_M \approx 0.45$ computed at $T = 0$ in the MSL, we find that $p_{\mathbf{R}\mathbf{R}'}^{singlet} \approx 0.60$ on these effectively coupled bonds. This value has to be compared with the value $\ln(2) \approx 0.69$ that is predicted for a one-dimensional Heisenberg chain using exact methods.^{35,36} We may thus interpret the MSL as a crystal of interacting filaments formed by the connected effectively coupled bonds. In this picture, spin excitations are deconfined fermions moving along these filaments. This may generalize the usual concept of valence bond crystal³⁷ where localized spin 1 excitations correspond to confined fermions.

Discussion.—Here we considered a model with only localized spins. However we know from previous works on heavy-fermions and cuprates that charge fluctuations play a crucial role in destabilizing AF states. In the context of cuprates, the AF phase of the insulating parent compounds corresponds to Q_{AF}^{II} . The SL phase introduced by Anderson *et al.*²⁷⁻³¹ corresponds to the homogeneous correlated state associated here with $\Phi_2 \neq 0$. One crucial specificity of this SL-scenario for superconductivity in cuprates relies on the two-dimensionality of the system. Stabilizing a SL state in 3D is commonly thought to be more tricky in view of the fact that the corresponding linear SW correction remains finite within a large S approach. Nevertheless, we have shown how frustration in the BCT-lattice can enhance the critical value S_c that, in some sense, characterizes the weakness of AF order against SW fluctuations. In connection with this weakening, we have identified various SL-phases that can be stabilized when n is larger than a relatively small critical value. This opens completely new perspectives for the realization of unconventional electronic quantum orderings in 3D. In particular, these results suggest that the BCT-lattice structure can play a central role in crystalline materials like the 122 and some cuprates in spite of numerous phases emerging in these systems. Indeed, the very rich phase diagram depicted in figures 2 and 3 could provide a unifying framework for understanding and analyzing the intersite correlations in these compounds. The number n may be considered as an effective parameter related to the electronic orbital degeneracy, that could be phenomenologically increased or decreased by charge fluctuations or crystal field effects. Considering a given compound, n might also be effectively decreased by applying an external magnetic field. Similarly, a tuning of the model parameters p_2 and p_3 may phenomenologically account for some effects of applying pressure.³⁴ For example, this scenario could explain two different AF instabilities of the HO phase that are observed experimentally in URu₂Si₂: assuming that HO is a MSL order, and applying a finite pressure this corresponds to increasing J_1 for a fixed n (see fig. 3), leading to a commensurate AF instability characterized by Q_{AF}^I as observed experimentally.^{4,5} Alternatively, applying a magnetic field without pressure corresponds to lowering the effective value of n for fixed p_2 and p_3 : the MSL (HO) is destabilized to an incommensurate AF. Interestingly, using different numerical values of J_1 , J_2 , and J_3 obtained from different fits of Inelastic Neu-

tron Scattering datas, our scenario predicts an instability from MSL to $\mathbf{Q}_{\text{inc}}^{\text{III}} = (\Upsilon_3, 0, 0)$ with $\Upsilon_3 \approx 0.69$ (from³⁸), 0.66 (from³⁹), 0.69 (from²³) and 0.65 (from⁴⁰). This scenario could be tested experimentally since it predicts that the AF order $\mathbf{Q}_{\text{inc}}^{\text{III}}$ could be continuously tuned to $\mathbf{Q}_{\text{AF}}^{\text{I}}$ by applying pressure on URu₂Si₂ under a high magnetic field.

Invoking the SL instabilities described in this letter we may also generalize to 3D systems the spin-fluctuation pairing mechanism that was proposed in terms of gauge transformations in.^{41,42} Here, the link between the BCT lattice structure and the superconducting order parameter is natural. It can be tested experimentally since we predict that the symmetries of the resulting superconducting order parameters will result from the point group symmetries of the SL, which may correspond to inplane pairing related to Φ_2 or Φ_3 or fully 3D pairing associated with Φ_1 . This SL mechanism driven by frustration on the BCT lattice may also be tested for the heavy-fermion superconductors CeRu₂Si₂ and CePd₂Si₂, but in these systems valence fluctuation effects need to be carefully included. The possible formation of a MSL could also

give rise to a commensurately ordered pairing that would break the BCT-symmetry down to simple tetragonal. Such a modulated pairing unconventional scenario could be tested with the superconducting instability observed in URu₂Si₂ inside the HO phase. Alternatively, even if the chiral SL order was found here to be less stable than the MSL, an opposite result could occur by including charge fluctuations.

ACKNOWLEDGMENTS

We acknowledge the financial support of Capes-Cofecub Ph 743-12. CT is *bolsista Capes*. This research was also supported in part by the Brazilian Ministry of Science, Technology and Innovation (MCTI) and the Conselho Nacional de Desenvolvimento Científico e Tecnológico (CNPq). Research carried out with the aid of the Computer System of High Performance of the International Institute of Physics-UFRN, Natal, Brazil. The authors are grateful to Frédéric Bourdarot for useful discussions.

- ¹ C. Kittel, *Introduction to Solid State Physics - eighth edition* (John Wiley & Sons, 2005).
- ² G. Stewart, *Review of Modern Physics* **56**, 755 (1984).
- ³ P. Fulde, P. Thalmeier, and G. Zwirnagl, *Solid State Physics: Advances In Research and Applications* **60**, 1 (2006).
- ⁴ T. Palstra, A. Menovsky, J. Vandenberg, A. Dirkmaat, P. Kes, G. Nieuwenhuys, and J. Mydosh, *Physical Review Letters* **55**, 2727 (1985).
- ⁵ J. Mydosh and P. Oppeneer, *Review of Modern Physics* **83**, 1301 (2011).
- ⁶ J. Custers, P. Gegenwart, H. Wilhelm, K. Neumaier, Y. Tokiwa, O. Trovarelli, C. Geibel, F. Steglich, C. Pépin, and P. Coleman, *Nature* **424**, 524 (2003).
- ⁷ S. Friedemann, T. Westerkamp, M. Brando, N. Oeschler, S. Wirth, P. Gegenwart, C. Krellner, C. Geibel, and F. Steglich, *Nature Physics* **5**, 465 (2009).
- ⁸ J. Mignot, J. Flouquet, P. Haen, F. Lapierre, L. Puech, and J. Voiron, *Journal of Magnetism and Magnetic Materials* **76-7**, 97 (1988).
- ⁹ W. Knafo, S. Raymond, P. Lejay, and J. Flouquet, *Nature Physics* **5**, 753 (2009).
- ¹⁰ F. Steglich, J. Aarts, C. Bredl, W. Lieke, D. Meschede, W. Franz, and H. Schafer, *Physical Review Letters* **43**, 1892 (1979).
- ¹¹ N. Mathur, F. Grosche, S. Julian, I. Walker, D. Freye, R. Haselwimmer, and G. Lonzarich, *Nature* **394**, 39 (1998).
- ¹² A. Demuer, D. Jaccard, I. Sheikin, S. Raymond, B. Salce, J. Thomasson, D. Braithwaite, and J. Flouquet, *Journal of Physics - Condensed matter* **13**, 9335 (2001).
- ¹³ S. Kawarazaki, M. Sato, Y. Miyako, N. Chigusa, K. Watanabe, N. Metoki, Y. Koike, and M. Nishi, *Physical Review B* **61**, 4167 (2000).
- ¹⁴ J. Bednorz and K. Muller, *Zeitschrift Fur Physik B-condensed Matter* **64**, 189 (1986).
- ¹⁵ J. Villain, *J. Phys. Chem. Solids* **11**, 303 (1959).
- ¹⁶ H. Diep, *Physical Review B* **40**, 741 (1989).
- ¹⁷ H. Diep, *Physical Review B* **39**, 397 (1989).
- ¹⁸ E. Rastelli, S. Sedazzari, and A. Tassi, *Journal of Physics-condensed Matter* **1**, 4735 (1989).
- ¹⁹ E. Rastelli, S. Sedazzari, and A. Tassi, *Journal of Physics-condensed Matter* **2**, 8935 (1990).
- ²⁰ R. Quartu and H. Diep, *Journal of Magnetism and Magnetic Materials* **182**, 38 (1998).
- ²¹ D. Loison, *Physica A* **275**, 207 (2000).
- ²² A. Sorokin and A. Syromyatnikov, *Journal of Experimental and Theoretical Physics* **113**, 673 (2011).
- ²³ K. Sugiyama, H. Fuke, K. Kindo, K. Shimoata, A. Menovsky, J. Mydosh, and M. Date, *Journal of the Physical Society of Japan* **59**, 3331 (1990).
- ²⁴ A. Chubukov, *Journal of Physics C: Solid State Physics* **17**, L991 (1984).
- ²⁵ P. Chandra and B. Douçot, *Phys. Rev. B* **38**, 9335(R) (1988).
- ²⁶ A. Aharony and B. Huberman, *Journal of physics C - Solid state physics* **9**, L465 (1976).
- ²⁷ P. Fazekas and P. Anderson, *Philosophical magazine* **30**, 423 (1974).
- ²⁸ P. Anderson, G. Baskaran, Z. Zou, and T. Hsu, *Physical Review Letters* **58**, 2790 (1987).
- ²⁹ G. Baskaran, Z. Zou, and P. Anderson, *Solid state communications* **63**, 973 (1987).
- ³⁰ T. Rice, S. Gopalan, and M. Sigrist, *Europhysics Letters* **23**, 445 (1993).
- ³¹ X. Wen and P. Lee, *Physical Review Letters* **76**, 503 (1996).
- ³² I. Affleck and J. Marston, *Phys. Rev. B* **37**, 3774 (1988).
- ³³ C. Pépin, M. Norman, S. Burdin, and A. Ferraz, *Physical Review Letters* **106**, 106601 (2011).
- ³⁴ C. Thomas, S. Burdin, C. Pépin, and A. Ferraz, *Physical Review B* **87**, 014422 (2013).
- ³⁵ H. Bethe, *Zeitschrift fur Physik* **71**, 205 (1931).
- ³⁶ U. Schollwöck, *Review of Modern Physics* **77**, 259 (2005).
- ³⁷ C. Lacroix, P. Mendels, and F. Mila, eds., *Introduction to Frustrated Magnetism*, Series in Solid-State Sciences, Vol. 164 (Springer, 2011) materials, Experiments, Theory.
- ³⁸ C. Broholm, H. Lin, P. Matthews, T. Mason, W. Buyers, M. Collins, A. Menovsky, J. Mydosh, and J. Kjems, *Physical*

- Review B **43**, 12809 (1991).
- ³⁹ H. Kusunose, Journal of the physical society of Japan **81**, 023704 (2012).
- ⁴⁰ F. Bourdarot, *Une autre vue sur URu₂Si₂* (Habilitation thesis, Grenoble, 2013).
- ⁴¹ P. A. Lee, N. Nagaosa, and X. G. Wen, Reviews of Modern Physics **78**, 17 (2006).
- ⁴² X.-G. Wen, *Quantum Field Theory of Many-Body Systems: From the Origin of Sound to an Origin of Light and Electrons*, Oxford Graduate Texts (Oxford University Press, 2004).